USING A TOWED ARRAY TO LOCALISE AND QUANTIFY UNDERWATER SOUND RADIATED BY THE TOW-VESSEL

Alec J. Duncan(1), Darryl R McMahon(2)

(1) Centre for Marine Science and Technology, Curtin University of Technology, Australia
(2) Defence Science and Technology Organisation, Maritime Operations Division, Australia

Abstract

This paper presents the results of a study aimed at determining the feasibility of using a towed array of hydrophones to localise and quantify sound sources on the tow-vessel. The method requires the tow-vessel to execute a manoeuvre in order to bring the array into a suitable geometry to allow it to image the tow-vessel. Previous work has focussed on a scenario where the tow-vessel executes a U-turn manoeuvre, resulting in rapid relative motion between the tow-vessel and hydrophones. In this paper a simulation is used to compare the performance of different beamforming algorithms in a scenario where the tow-vessel executes a constant radius turn. This scenario has the advantage of allowing longer integration times than the U-turn manoeuvre.

Introduction

It is advantageous for Navy vessels, particularly submarines, to have a means of measuring their own acoustic signature and localising the primary sources of radiated acoustic noise that contribute to that signature. This is conventionally done using fixed acoustic ranges, which require the vessel to divert to wherever the range is located, or air-dropped sonobuoys, which require a cooperating aircraft. This paper builds on previous work reported in [1-3] aimed at determining the feasibility of using the vessel's own towed hydrophone array to make acoustic signature and source localisation measurements without the need for fixed ranges or sonobuoys.

The feasibility of performing this type of measurement was demonstrated in the work described in [1] which included a field trial in which a surface vessel towing an array of hydrophones carried out a series of U-turn manoeuvres. A disadvantage of the U-turn manoeuvre is that there is rapid relative motion between the hydrophones and the vessel when the geometry is most favourable for beamforming (when the acoustic section is broadside to the vessel). This makes tracking the hydrophone locations extremely critical and also limits the integration time available for beamforming.

The work described in this paper uses simulations to investigate an alternative scenario in which the tow-vessel executes a constant radius turn. This results in the acoustic section of the array taking up a stable position relative to the vessel, reducing the hydrophone tracking requirements and allowing for longer integration times. The performance of several array processing algorithms are investigated for three acoustic source configurations: a single point source, a pair of coherent sources, and a rectangular piston.

Test Scenario

Vessel and towed array

The tow-vessel was assumed to be 100 m long and operating at a depth of 100 m below the water surface. The simulated manoeuvre consisted of a 225 m radius turn to starboard at a speed of 1 m/s.

The towed array used in this simulation had an overall length of 750 m and consisted of four sections: a tow-cable, a forward vibration isolation module, an acoustic section, and an aft vibration isolation module. The diameter and density of each section were typical of a towed array and the water density was 1025 kg.m^{-3}. The acoustic section was 150 m long and contained 64 equally spaced hydrophones spread over its entire length, giving a hydrophone spacing of 2.381 m. The hydrophones were assumed to be omni-directional at all frequencies.
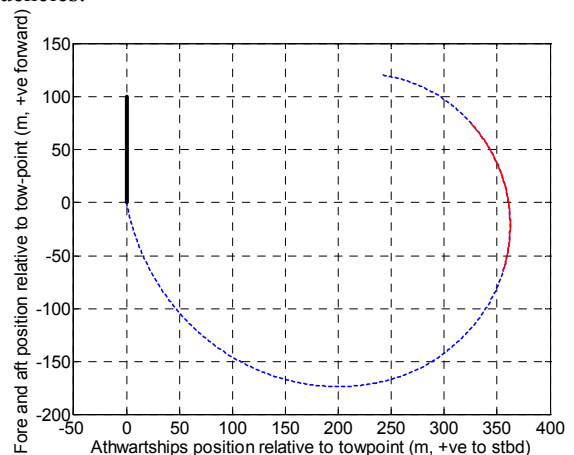

Figure 1   Steady-state horizontal plane array shape relative to tow-vessel. The thick black line is the centre-line of the tow-vessel and the solid red line is the acoustic section of the array.

The steady-state array shape was calculated using the program described in [2] and is plotted in figures 1 and 2.
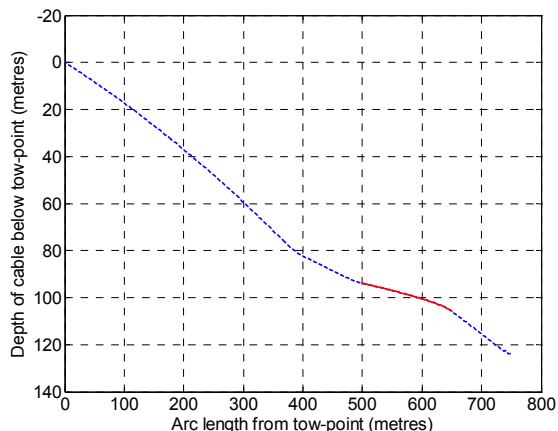

Figure 2 Steady-state vertical plane array shape relative to tow-vessel. Solid red line is the acoustic section of the array.

Sources

The results reported in this paper are for three different source configurations: a point source located at $X = 50$ m, two equal amplitude coherent point sources located at $X = 42.5$ m and $X = 57.5$ m, and a 15 m wide, 2 m high rectangular piston located at $X = 50$ m. All sources were modelled as machinery noise sources with spectra consisting of a 5 Hz fundamental and a series of equal amplitude harmonics spanning the range 5 Hz to 900 Hz. The phases of the harmonics were random and taken from a uniform distribution from 0 to 2π radians.

The algorithms used to simulate the sources are described in [1] and [3]. Propagation calculations were carried out using the program described in [1] assuming spherical spreading. Surface reflections were included where required using the image method, in which each physical source was accompanied by its mirror image in the sea surface plane.

Spatially and temporally uncorrelated Gaussian noise was added to the simulated received signals to give an average signal to noise ratio of 0 dB at each hydrophone. Temporally uncorrelated (white) noise was used so that the signal to noise ratio was the same at all frequencies. A 0 dB signal to noise ratio is quite realistic for an acoustic section 350 m from the tow-vessel, making it necessary to utilize the directional gain of the towed array in order to obtain good source level estimates.

Array processing algorithms

The array processing algorithms used in this comparison were all frequency domain algorithms. A column vector, $\mathbf{x}$, with one element for each of the N hydrophones, represents the output of the array at a particular frequency. The elements of $\mathbf{x}$ are complex numbers representing the magnitude and phase of the received signal.

The response of the array to a point source at location l, in the absence of noise, is called the steering vector, $\mathbf{a}_l$. When dealing L source locations the steering vectors can be combined into a steering matrix:

$$\mathbf{A} = \begin{bmatrix} \mathbf{a}_1 & \mathbf{a}_2 & \cdots & \mathbf{a}_L \end{bmatrix} \tag{1}$$

Least Squares Minimum Constrained (LSMC)

The output of a conventional beamformer is given by:

$$y = \mathbf{w}^H \mathbf{x} \tag{2}$$

where $\mathbf{w}$ is an N element vector of complex weights and the superscript H denotes the Hermitian transpose (complex conjugate of the transpose).

In [1] it was shown that improved results could be obtained by using a weight vector that minimised the response of the beamformer to sources at locations on the vessel away from the focal point subject to a penalty on the white noise gain and a constraint of unity gain for a source at the focal point. This requirement led to the following expression for the weight vector:

$$\mathbf{w} = \frac{\mathbf{M}^{-1}\mathbf{a}_0}{\mathbf{a}_0^H \mathbf{M}^{-1}\mathbf{a}_0} \tag{3}$$

where

$$\mathbf{M} = \mathbf{A}\mathbf{A}^H + \beta\mathbf{I}$$

In this expression the steering matrix, $\mathbf{A}$, contains steering vectors corresponding to locations at which it is desired to minimise the array response, $\mathbf{a}_0$ is the steering vector for the focal point, and β controls the relative weight given to minimising the white noise gain.

Minimum Variance Distortionless Response (MVDR)

This beamformer works by minimising the output power (variance) of the beamformer subject to the constraint of unity gain in the look direction (far-field case) or for a source at the focal point (near-field case). The weight vector therefore depends on the array output, making it a data dependent, or adaptive, beamformer.

A version of the MVDR beamformer capable of dealing with near-field sources moving rapidly relative to the array was derived in [1]. Although the scenario simulated here does not include any relative motion between the array and the vessel, in practice there would be some residual motion and it would be necessary to use the dynamic version of the algorithm.

Firstly, a transformation is applied to the array output vector as follows:

$$\mathbf{z}_k = \mathbf{T}_k \mathbf{x}_k \tag{4}$$

where the subscript k represents the snapshot number and $\mathbf{T}_k$ is the diagonal transformation matrix:

$$\mathbf{T}_k = \begin{bmatrix} a_{1,k}/a_{1,1} & & \\ & \ddots & \\ & & a_{N,k}/a_{N,1} \end{bmatrix} \quad (5)$$

Here $a_{n,k}$ is the nth element of the steering vector for the desired focal point at the midpoint of snapshot k. The effect of this transformation is to produce the same output at snapshot k for a source at the focal point as would have been produced if the array had stayed at the position it was in at the midpoint of the first snapshot. The effective steering vector and required weight vector are therefore constant and the beamformer output power can be computed using the usual MVDR formula:

$$\Pi = \frac{1}{\mathbf{a}_1^H \hat{\mathbf{R}}_z^{-1} \mathbf{a}_1} \quad (6)$$

where Π is the beamformer output power, $\mathbf{a}_1$ is the steering vector for the desired focal point at the midpoint of the first snapshot and $\hat{\mathbf{R}}_z$ is an estimate of the covariance matrix of $\mathbf{z}$ given by:

$$\hat{\mathbf{R}}_z = \frac{1}{K} \sum_{k=1}^{K} \mathbf{z}_k \mathbf{z}_k^H + \varepsilon \mathbf{I} \quad (7)$$

Here K is the number of snapshots and ε is a positive number that controls the amount of diagonal loading. Diagonal loading reduces the number of snapshots required to obtain a useable covariance matrix estimate.

Spatially Smoothed MVDR

The MVDR beamformer has the disadvantage that the presence of two or more coherent sources can lead to partial or complete cancellation of the desired output ([4]). In this context two sources are coherent if one produces a signal that is a delayed and scaled replica of the signal produced by the other.

This is of concern when attempting to image vessel noise sources because coherent sources can arise when noise from a particular piece of machinery is transmitted to the outer hull via several structural paths. In addition a spatially extended source can occur when mechanical vibrations excite hull plate flexural vibrations, yielding what is effectively an array of closely spaced coherent sources.

A common method of reducing the effect of source coherence is to carry out spatial smoothing ([4], [5]). In the far-field, uniform line array case this involves dividing the array into a number of smaller, overlapping sub-arrays. The covariance matrix for each sub-array is calculated and these are averaged to produce the covariance matrix that is used in the output power calculation.

Applying this method to the near-field, curved array case was complicated by the fact that sub-array steering vectors are no longer the same except for a phase term. This problem was overcome by using the transformation method described earlier in the context of dealing with moving arrays.

The transformation is now:

$$\mathbf{z}_{k,q} = \mathbf{T}_{k,q} \mathbf{x}_{k,q} \quad (8)$$

where the subscript k represents the snapshot number and q represents the sub-array number. $\mathbf{x}_{k,q}$ is the sub-array output vector and $\mathbf{T}_{k,q}$ is the diagonal transformation matrix:

$$\mathbf{T}_{k,q} = \begin{bmatrix} a_{1,k,q}/a_{1,1,1} & & \\ & \ddots & \\ & & a_{N',k,q}/a_{N',1,1} \end{bmatrix} \quad (9)$$

Here N' is the number of hydrophones in the sub-array and $a_{n,k,q}$ is the nth element of the sub-array steering vector for the desired focal point for snapshot k and sub-array q. The covariance matrix is calculated from:

$$\hat{\mathbf{R}}_z = \frac{1}{KQ} \sum_{k=1}^{K} \sum_{q=1}^{Q} \mathbf{z}_{k,q} \mathbf{z}_{k,q}^H + \varepsilon \mathbf{I} \quad (10)$$

Regularised inversion processor

A detailed derivation of the regularised inversion (RI) processor is given in [1] and only a brief outline is given here.

Let $\mathbf{s}$ be a vector of source complex amplitudes at specified locations, and $\mathbf{A}$ be the steering matrix for these locations. The array output vector is then given by:

$$\mathbf{x} = \mathbf{A}\mathbf{s} + \mathbf{n} \quad (11)$$

where $\mathbf{n}$ is a noise vector.

In principle this equation can be solved for $\mathbf{s}$ using standard least squares techniques, but the equation is generally ill-conditioned (there are many different source vectors that will give the same array output) and it is necessary to use some form of regularisation. The regularisation used here was to minimise the total signal power, which is proportional to $\mathbf{s}^H \mathbf{s}$. This leads to:

$$\mathbf{s} = \left(\mathbf{A}^H \mathbf{A} + \gamma I \right)^{-1} \mathbf{A}^H \mathbf{x} \quad (12)$$

where γ is a trade-off parameter that controls the relative weight given to minimising the signal power compared to fitting the measured data and I is the identity matrix.

A major difference between this processor and the various beamforming methods described above is that it inverts for the set of source amplitudes that would generate an acoustic field consistent with the array data, whereas the beamformers focus on one point at a time and attempt to determine the acoustic power being emitted from the focal point while ignoring the effects of sources in other locations.

Results

Figures 3 to 5 show the results of applying the LSMC beamformer, the RI processor and the smoothed MVDR beamformer to simulated data for a pair of equal amplitude coherent point sources separated by 15 m. The true source spectral level was 176 dB re $1\mu Pa^2$/Hz @ 1 m and the simulated data were computed using spherical spreading.

As expected, the unsmoothed MVDR processor performed very poorly for this scenario, with almost total cancellation of the coherent sources, and has not been plotted.

The LSMC beamformer was able to resolve the two sources at frequencies above 250 Hz and gave good estimates of the source levels.

The RI processor had similar spatial resolution but its different normalisation resulted in source levels that increased with frequency. This is because the changing spatial resolution meant that the number of the RI processor's assumed source locations that contributed significantly to the measured field reduced as the frequency increased, and therefore the source levels required to match the measured field increased.

The smoothed MVDR beamformer localised the sources more accurately than the other algorithms at high frequencies, but was no better at separating the sources at low frequencies.
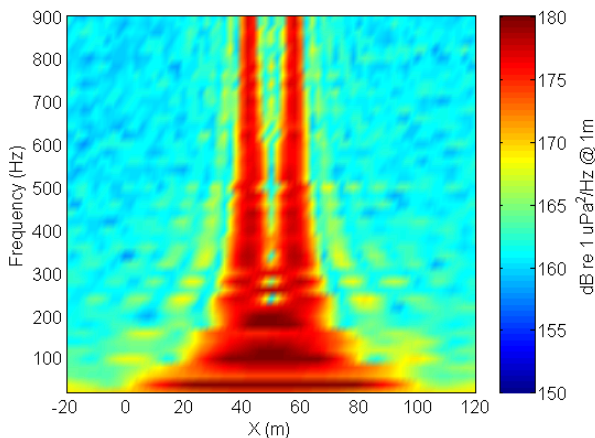

Figure 3   Output of LSMC beamformer for two coherent point sources.

Results for the 15 m wide rectangular piston source are shown in figures 6 and 8. The LSMC beamformer produced a good estimate of the source width at high frequencies but, because of its limited spatial resolution, overestimated the source width at low frequencies. The estimated source level decreased with increasing frequency, which was a consequence of the beamformer resolution becoming smaller than the physical width of the source.
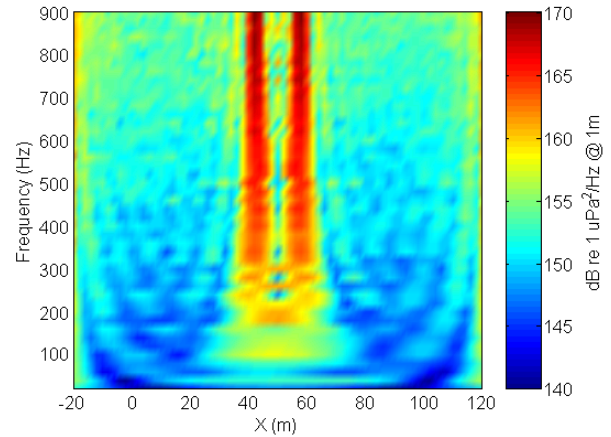

Figure 4   Output of RI processor for two coherent point sources.
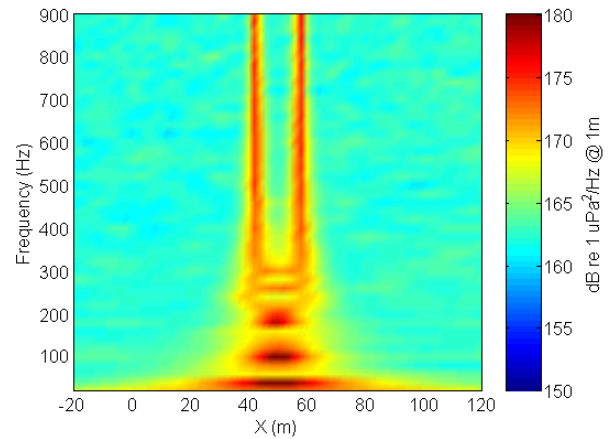

Figure 5   Output of smoothed MVDR beamformer for two coherent point sources.

The RI processor produced a slightly better estimate of the physical width of the source and also gave source level estimates that were largely independent of frequency above 250 Hz.

The smoothed MVDR beamformer performed poorly and suffered from almost complete cancellation above 350 Hz. This is a consequence of the limited ability of spatial averaging to decorrelate very close sources. When imaging an extended source the beamformer treats adjacent parts of the source as distinct, coherent sources, with a spacing determined by the beamformer's spatial resolution. At high frequencies this resulted in the rectangular piston being treated as many, closely spaced,

coherent sources, which the spatial averaging was unable to decorrelate, and the MVDR algorithm therefore cancelled.
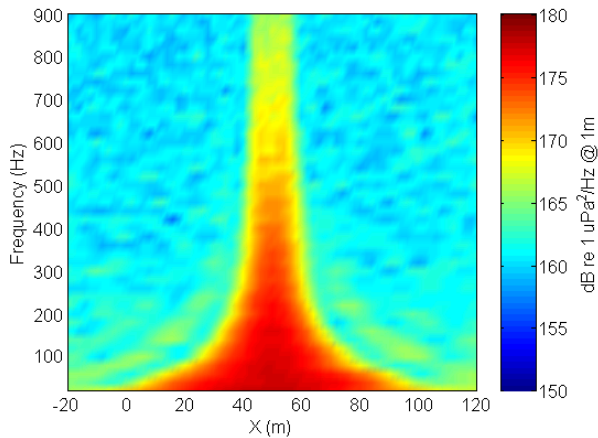

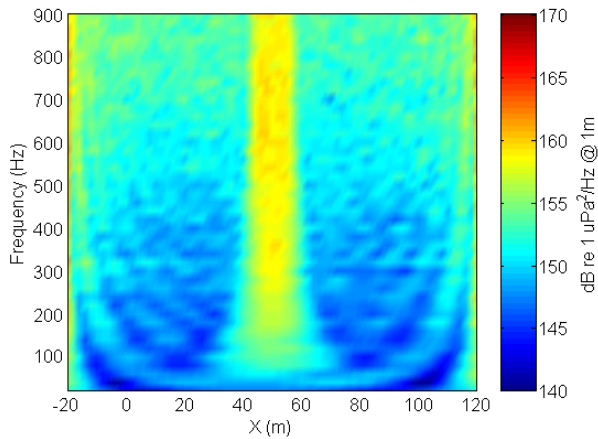Figure 6   Output of LSMC beamformer for rectangular piston source.

Figure 7   Output of RI processor for rectangular piston source.
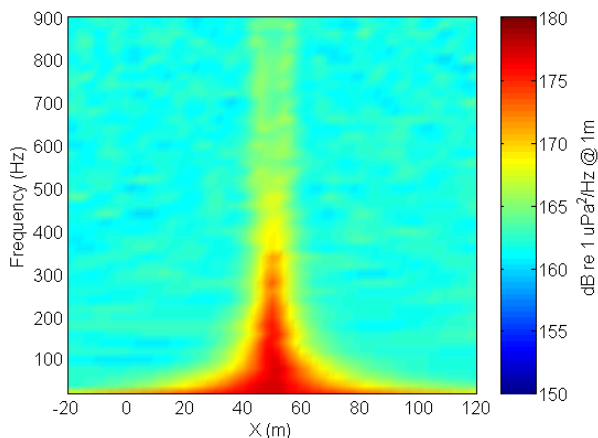

Figure 8   Output of smoothed MVDR beamformer for rectangular piston source.

Figure 9 shows the output of the LSMC beamformer for a single point source in a situation where the simulation included the sea surface reflection but the beamformer steering vectors were calculated assuming spherical spreading. The beamformer output in this situation had significant sidelobes and low frequency distortions, and overestimated the source level. Figure 10 shows the result when the steering vector calculation took account of the surface reflection, which removed the artefacts and gave more accurate source level estimates.
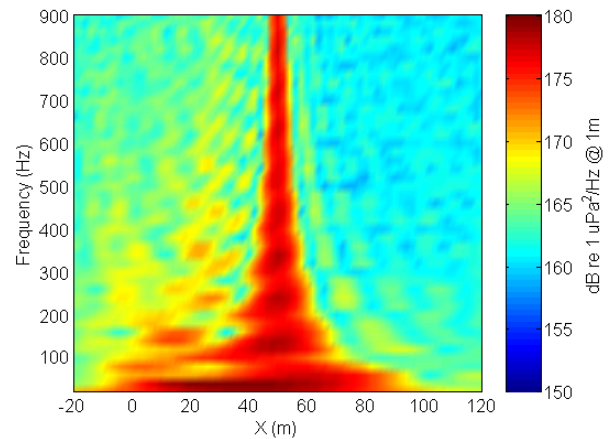

Figure 9   Output of LSMC beamformer for a single point source. Simulation includes surface reflection but steering vectors assume spherical spreading.
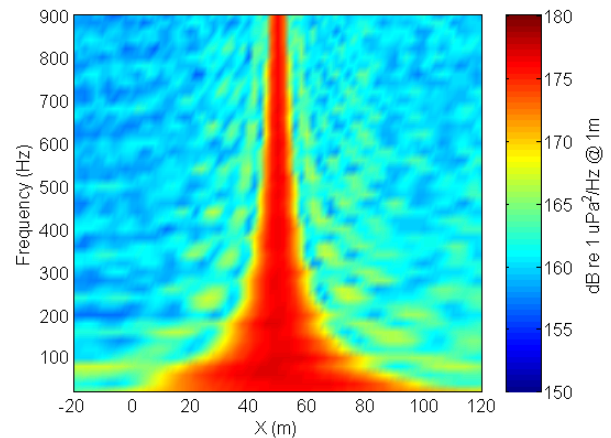

Figure 10   Output of LSMC beamformer for single point source when both simulation and steering vector calculation include surface reflection.

Conclusions

The LSMC beamformer and RI processor provided good performance with all source types and were better suited to this application than either the smoothed or unsmoothed MVDR beamformers. The smoothed MVDR beamformer was more generally applicable than the unsmoothed MVDR beamformer but performed

poorly with extended sources. When applied to point sources it had better apparent spatial resolution at high frequencies, but was no better at separating two closely spaced sources at low frequencies than the LSMC beamformer.

The spatial resolution of the RI processor was similar to that of the LSMC beamformer. The main difference between the results produced by these two algorithms was that the output of the LSMC beamformer was easier to interpret for point sources, because it gave a direct estimate of the source level, whereas the output of the RI processor was easier to interpret for extended sources, because it showed the contribution of each part of the source to the measured field.

The particular regularisation method used for RI found the source amplitude distribution that fitted the measured data while minimising the total signal power. This scheme favoured a smooth distribution of source amplitudes, resulting in poor performance with point sources at low frequencies. Alternative regularisation schemes are being investigated that may lead to improved performance in this situation.

References

[1] Duncan, AJ, "The measurement of the underwater acoustic noise radiated by a vessel using the vessel's own towed array", PhD, Curtin University of Technology, 2003.

[2] Gourlay, T and Duncan, AJ, "Steady-state towed array shape calculation for a circle manoeuvre", Centre for Marine Science and Technology, Curtin University of Technology, Report No. C2004-1, 2004.

[3] Duncan, AJ, "An approximate method for simulating the acoustic radiation from extended hull areas", Centre for Marine Science and Technology, Curtin University of Technology, Report No. C2004-17, 2004.

[4] Reddy, VU, Paulraj, A, and Kailath, T, "Performance analysis of the optimum beamformer in the presence of correlated sources and its behaviour under spatial smoothing", *IEEE transactions on Acoustics, Speech and Signal Processing* ASSP-35(7): 927-936, 1987.

[5] Krim, H and Veberg, M, "Two decades of array signal processing research: The parametric approach", *IEEE signal processing magazine*: 67-94, 1996.